AFRL-ML-WP-TP-2007-549

MECHANISM OF HYDROGEN PRODUCTION IN [Fe-Fe]-HYDROGENASE: A DENSITY FUNCTIONAL THEORY STUDY (POSTPRINT)

Ruth Pachter

Hardened Materials Branch
Survivability and Sensor Materials Division

MARCH 2007

STINFO COPY

AIR FORCE RESEARCH LABORATORY
MATERIALS AND MANUFACTURING DIRECTORATE
WRIGHT-PATTERSON AIR FORCE BASE, OH 45433-7750
AIR FORCE MATERIEL COMMAND
UNITED STATES AIR FORCE

NOTICE AND SIGNATURE PAGE

Using Government drawings, specifications, or other data included in this document for any purpose other than Government procurement does not in any way obligate the U.S. Government. The fact that the Government formulated or supplied the drawings, specifications, or other data does not license the holder or any other person or corporation; or convey any rights or permission to manufacture, use, or sell any patented invention that may relate to them.

This report was cleared for public release by the Air Force Research Laboratory Wright Site (AFRL/WS) Public Affairs Office and is available to the general public, including foreign nationals. Copies may be obtained from the Defense Technical Information Center (DTIC) (http://www.dtic.mil).

AFRL-ML-WP-TP-2007-549 HAS BEEN REVIEWED AND IS APPROVED FOR PUBLICATION IN ACCORDANCE WITH ASSIGNED DISTRIBUTION STATEMENT.

*//Signature//   //Signature//

RUTH PACHTER, Ph.D.   MARK S. FORTE, Acting Chief
Computational Materials Research   Hardened Materials Branch
Exploratory Development   Survivability and Sensor Materials Division
Hardened Materials Branch

//Signature//

TIM J. SCHUMACHER, Chief
Survivability and Sensor Materials Division

This report is published in the interest of scientific and technical information exchange, and its publication does not constitute the Government's approval or disapproval of its ideas or findings.

*Disseminated copies will show "//Signature//" stamped or typed above the signature blocks.

REPORT DOCUMENTATION PAGE

1. REPORT DATE *(DD-MM-YY)*	2. REPORT TYPE	3. DATES COVERED *(From - To)*
March 2007	Journal Article Postprint	

4. TITLE AND SUBTITLE

MECHANISM OF HYDROGEN PRODUCTION IN [Fe-Fe]-HYDROGENASE: A DENSITY FUNCTIONAL THEORY STUDY (POSTPRINT)

5a. CONTRACT NUMBER
In-house

5b. GRANT NUMBER

5c. PROGRAM ELEMENT NUMBER
62102F

6. AUTHOR(S)

Steven Trohalaki (General Dynamics Information Technology, Inc.)
Ruth Pachter (AFRL/MLPJE)

5d. PROJECT NUMBER
4348

5e. TASK NUMBER
RG

5f. WORK UNIT NUMBER
M08R1000

7. PERFORMING ORGANIZATION NAME(S) AND ADDRESS(ES)

General Dynamics Information
  Technology, Inc.
5100 Springfield Pike, Suite 509
Dayton, OH 45431-1264

Hardened Materials Branch (AFRL/MLPJE)
Survivability and Sensor Materials Division
Materials and Manufacturing Directorate
Wright-Patterson Air Force Base, OH 45433-7750
Air Force Materiel Command, United States Air Force

8. PERFORMING ORGANIZATION REPORT NUMBER
AFRL-ML-WP-TP-2007-549

9. SPONSORING/MONITORING AGENCY NAME(S) AND ADDRESS(ES)

Air Force Research Laboratory
Materials and Manufacturing Directorate
Wright-Patterson Air Force Base, OH 45433-7750
Air Force Materiel Command
United States Air Force

10. SPONSORING/MONITORING AGENCY ACRONYM(S)
AFRL/MLPJE

11. SPONSORING/MONITORING AGENCY REPORT NUMBER(S)
AFRL-ML-WP-TP-2007-549

12. DISTRIBUTION/AVAILABILITY STATEMENT
Approved for public release; distribution unlimited.

13. SUPPLEMENTARY NOTES

PAO Case Number: AFRL/WS 07-0177, 29 Jan 2007. Paper contains color.

14. ABSTRACT
[Fe-Fe]-hydrogenases are a class of metalloenzymes that catalyze the production of H2 from two protons and two electrons. In this work, we used density functional theory (DFT) calculations to analyze the mechanism of hydrogen production, providing insight into the role of the intermediates in the catalysis. We also validated the exchange-correlation functional applied within DFT for model compounds of the active site in [Fe-Fe]-hydrogenase, enabling us a reliable application for understanding previously established hydrogen production hypotheses, as well as providing a starting point for a future investigation of the effects of the protein environment on the catalytic mechanism of [Fe-Fe]-hydrogenases.

15. SUBJECT TERMS

16. SECURITY CLASSIFICATION OF:			17. LIMITATION OF ABSTRACT:	18. NUMBER OF PAGES	19a. NAME OF RESPONSIBLE PERSON (Monitor)
a. REPORT Unclassified	**b. ABSTRACT** Unclassified	**c. THIS PAGE** Unclassified	SAR	16	Ruth Pachter
					19b. TELEPHONE NUMBER *(Include Area Code)* N/A

Mechanism of Hydrogen Production in [Fe−Fe]-Hydrogenase: A Density Functional Theory Study

Steven Trohalaki*,†,‡ and Ruth Pachter*,†

Air Force Research Laboratory, Materials & Manufacturing Directorate,
Wright-Patterson Air Force Base, Ohio 45433-7702, and General Dynamics Information Technology, Inc.,
5100 Springfield Pike, Suite 509, Dayton, Ohio 45431-1264

[Fe−Fe]-hydrogenases are a class of metalloenzymes that catalyze the production of H_2 from two protons and two electrons. In this work, we used density functional theory (DFT) calculations to analyze the mechanism of hydrogen production, providing insight into the role of the intermediates in the catalysis. We also validated the exchange-correlation functional applied within DFT for model compounds of the active site in [Fe−Fe]-hydrogenase, enabling us a reliable application for understanding previously established hydrogen production hypotheses, as well as providing a starting point for a future investigation of the effects of the protein environment on the catalytic mechanism of [Fe−Fe]-hydrogenases.

Introduction

Recently, Prince and Kheshgi[1] assessed the potential efficiency of photobiological hydrogen production[2] as a renewable fuel, regarding the maximal energetic efficiency when using hydrogenases. It was noted that additional improvements in hydrogen generation at the biochemical level are required.[2] In our first step toward understanding the mechanism, we explored all-iron hydrogenases. The active-site domains of the all-iron hydrogenases from the sulfate-reducing microorganism *Desulfovibrio desulfuricans* (DdH)[3] and from the anaerobic soil microorganism *Clostridium pasteurianum* (CpI)[4,5] were found to be very similar,[6] although it has been inferred from the manner in which the crystals were obtained that the CpI structure represents an oxidized state and that the DdH structure represents a reduced state,[6] while Nicolet et al.[7] suggested that the DdH crystal represents a mixture of anaerobically oxidized and reduced states. The crystal structures for active sites in the [Fe−Fe]- and [Ni−Fe]-hydrogenases have also been shown to be surprisingly congruent,[7,8] reflecting convergent evolution.[9] However, although [Fe−Fe]-hydrogenases and [Ni−Fe]-hydrogenases readily catalyze the interconversion between the hydrogen molecule and two protons plus two electrons,[10] limitations, such as the sensitivity to O_2,[11,12] still need to be resolved. Moreover, an understanding of the dependence of the protein environment on the catalytic mechanism is still lacking, as recently reviewed.[9]

In order to gain insight into the catalytic activity of [Fe−Fe]-hydrogenases, a number of theoretical density functional theory (DFT) studies emerged,[13−23] focusing mostly on the Fe_2S_2

* Corresponding authors. Phone: (937) 255-9593 (S.T.), (937) 255-9689 (R.P.). FAX: (937) 255-3377 (S.T.), (937) 255-1128 (R.P.). E-mail: steven.trohalaki@wpafb.af.mil (S.T.), ruth.pachter@wpafb.af.mil (R.P.).
† Air Force Research Laboratory.
‡ General Dynamics Information Technology, Inc.

(1) Prince, R. C.; Kheshgi, H. S. The Photobiological Production of Hydrogen: Potential Efficiency and Effectiveness as a Renewable Fuel. *Crit. Rev. Microbiol.* **2005**, *13*, 19−31.

(2) Boichenko, V. A.; Greenbaum, E.; Seibert, M. *Hydrogen Production by Photosynthetic Microorganisms*; Imperial College Press: London, 2004; Vol. 2, pp 397−452.

(3) Nicolet, Y.; Piras, C.; Legrand, P.; Hatchikian, E. C.; Fontecilla-Camps, J. C. Desulfovibrio Desulfuricans Iron Hydrogenase: The Structure Shows Unusual Coordination to an Active Site Fe Binuclear Center. *Structure* **1999**, *7*, 13−23.

(4) Peters, J. W.; Lanzilotta, W. N.; Lemon, B. J.; Seefeldt, L. C. X-ray Crystal Structure of the Fe-Only Hydrogenase (CpI) from *Clostridium pasteurianum* to 1.8 Angstron Resolution. *Science* **1998**, *282*, 1853−1858.

(5) Nicolet, Y.; Lemon, B. J.; Fontecilla-Camps, J. C.; Peters, J. W. A Novel FeS Cluster in Fe-Only Hydrogenases. *Trends Biochem. Sci.* **2000**, *25*, 138−143.

(6) Peters, J. W. Structure and Mechanism of Iron-Only Hydrogenases. *Curr. Opin. Struct. Biol.* **1999**, *9*, 670−676.

(7) Nicolet, Y.; De Lacey, A. L.; Vernede, X.; Fernandez, V. M.; Hatchikian, E. C.; Fontecilla-Camps, J. C. Crystallographic and FTIR Spectroscopic Evidence of Changes in Fe Coordination upon Reduction of the Active Site of the Fe-Only Hydrogenase from Desulfovibrio desulfuricans. *J. Am. Chem. Soc.* **2001**, *123*, 1596−1601.

(8) Volbeda, A.; Fontecilla-Camps, J. C. The Active Site and Catalytic Mechanism of NiFe Hydrogenases. *Dalton Trans.* **2003**, 4030−4038.

(9) Armstrong, F. A. Hydrogenases: Active Site Puzzles and Progress. *Curr. Opin. Struct. Biol.* **2004**, *8*, 133−140.

(10) Cammack, R.; Frey, M.; Robson, R. L. *Hydrogen as a Fuel: Learning from Nature*; Taylor & Francis: London and New York, 2001.

(11) Ghirardi, M. L.; King, P. W.; Posewitz, M. C.; Maness, P. C.; Fedorov, A.; Kim, K.; Cohen, J.; Schulten, K.; Seibert, M. Approaches to Developing Biological H_2-Photoproducing Organisms and Processes. *Biochem. Soc. Trans.* **2005**, *33*, 70−72.

(12) Vincent, K. A.; Parkin, A.; Lenz, O.; Albracht, S. P. J.; Fontecilla-Camps, J. C.; Cammack, R.; Friedrich, B.; Armstrong, F. A. Electrochemical Definitions of O2 Sensitivity and Oxidative Inactivation in Hydrogenases. *J. Am. Chem. Soc.* **2005**, *127*, 18179−18189.

(13) Liu, Z.-P.; Hu, P. A Density Functional Theory Study on the Active Center of Fe-Only Hydrogenase: Characterization and Electronic Structure of the Redox States. *J. Am. Chem. Soc.* **2002**, *124*, 5175−5182.

(14) Liu, Z.-P.; Hu, P. Mechanism of H2 Metabolism on Fe-Only Hydrogenases. *J. Chem. Phys.* **2002**, *117*, 8177−8180.

(15) Bruschi, M.; Fantucci, P.; Gioia, L. D. DFT Investigation of Structural, Electronic, and Catalytic Properties of Diiron Complexes Related to the [2Fe]$_H$ Subcluster of Fe-Only Hydrogenases. *Inorg. Chem.* **2002**, *41*, 1421−1429.

(16) Bruschi, M.; Fantucci, P.; Gioia, L. D. Density Functional Theory Investigation of the Active Site of [Fe]-Hydrogenases: Effects of Redox State and Ligand Characteristics on Structural, Electronic, and Reactivity Properties of Complexes Related to the [2Fe]$_H$ Subcluster. *Inorg. Chem.* **2003**, *42*, 4773−4781.

(17) Bruschi, M.; Fantucci, P.; Gioia, L. D. Density Functional Theory Investigation of the Active Site of Fe-Hydrogenases. Systematic Study of the Effects of Redox State and Ligands Hardness on Structural and Electronic Properties of Complexes Related to the [2Fe]$_H$ Subcluster. *Inorg. Chem.* **2004**, *43*, 3733−3741.
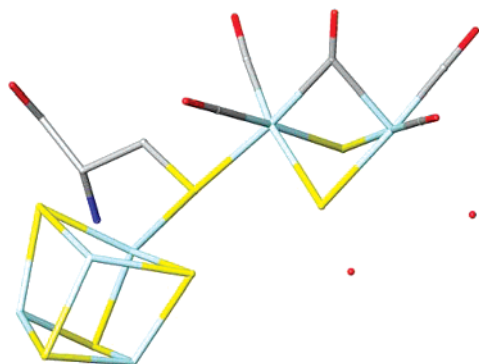
Figure 1. The [Fe−Fe]-hydrogenase active site from the CpI crystal structure, which consists of an Fe₂S₂ subcluster, termed [2Fe]ₕ, linked to a [4Fe-4S]ₕ subcluster through a cysteinyl sulfur. Here, the cysteine is included. Red, oxygen; yellow, sulfur; blue, nitrogen; aqua, iron; and gray, carbon.

subcluster in the active site (abbreviated [2Fe]ₕ), while excluding the remaining subcluster in the active site, namely, the Fe₄S₄ cubane (abbreviated [4Fe-4S]ₕ), which is linked to [2Fe]ₕ through a cysteinyl sulfur (see Figure 1). Considering both theory and experiment, Armstrong[9] outlined the relationships between different states of [2Fe]ₕ, addressing structure, mechanisms of activation, and hydrogen cycling (see Figure 3 in ref 9) as well as posing several questions.[9] In this work, we have modeled the intermediates in Armstrong's outline[9] as a starting point for elucidation of the mechanism and expanded on it by including an additionally oxidized species. We endeavor here to confirm this outline and provide insight into the questions posed. We also validated the exchange-correlation (x-c) functional to be applied within DFT for a model system for [Fe₂]ₕ and for two other model compounds for the CpI active site, enabling us a reliable application. The structural changes we calculated for the different functionals emphasize the importance of applying the appropriate level of theory, and thus our work will serve as the starting point for future investigations of the effects of the protein environment on the catalytic mechanism of [Fe−Fe]-hydrogenases.

Methods

DFT calculations at the BP86[24,25]/LACV3P**[26] and B3LYP[25,27,28]/LACV3P**[26] levels were performed with the software package

Figure 2. Model compounds **A**, **B**, and **C**.

Jaguar.[29] Note that the two Fe atoms in [2Fe]ₕ are termed proximal and distal (Feₚ and Fe_d), which refer to their proximity to the [4Fe−4S]ₕ subcluster (we also use subscripts p and d to indicate to which iron atom ligands are coordinated). The coordination geometry of [2Fe]ₕ with a carbonyl (CO_b) bridging the Fe atoms is that of two edge-bridged square pyramids; the CN, CO, and noncysteinyl sulfur atoms form the base, and the axial position is occupied by the bridging carbonyl, CO_b. In some unbridged structures, CO_b rotates ~180° around Fe_d but still occupies an axial position, resulting in an inverted square pyramid about Fe_d, although the two square pyramids still share an edge. We used a dihedral angle, ϕ_{CO}, to characterize the orientation of CO_b in [2Fe]ₕ; ϕ_{CO} is defined as X−Fe_d−Feₚ−CO_b, where X is the middle atom in either the propane or dimethyamine that bridges the noncysteinyl sulfur atoms.

First, three model compounds of the active site were considered in the calculations (**A**, **B**, and **C** in Figure 2): **A** is (μ-PDT)Fe₂-(CO)₃(CN)₂(CH₃S⁻) (**5** in ref 17); **B** is [Fe₂]ₕ based on the CpI X-ray structure[4] with CH₃S⁻ substituted for cysteine and the Fe₄S₄ cubane removed; **C** is [Fe₂]ₕ based on the CpI X-ray structure[4] coordinated to the Fe₄S₄ cubane through Cys503. Initial construction of model compounds **B**, **C**, and those in Armstrong's outline[9] (model compounds **1**−**8**) used the coordinates for residues 580, 581, and 503, from the CpI crystal structure,[4] that is, for [Fe₂]ₕ, the Fe₄S₄ cubane, and the cysteine, respectively. Hydrogen atoms were added as appropriate, and one of the two lone oxygen atoms in residue 580 was assumed to be a water molecule ligated to Fe_d. For **B**, **C**, and **1**−**3**, the following modifications were made: (1) One carbonyl group coordinated to Feₚ and one coordinated to Fe_d

(18) Cao, Z.; Hall, M. B. Modeling the Active Sites in Metalloenzymes. 3. Density Functional Calculations on Models for [Fe]-Hydrogenase: Structures and Vibrational Frequencies of the Observed Redox Forms and the Reaction Mechanism at the Diiron Active Center. *J. Am. Chem. Soc.* **2001**, *123*, 3734−3742.

(19) Popescu, C. V.; Münck, E. Electronic Structure of the H-Cluster in [Fe]-Hydrogenases. *J. Am. Chem. Soc.* **1999**, *121*, 7877−7884.

(20) Zampella, G.; Bruschi, M.; Fantucci, P.; Razavet, M.; Pickett, C. J.; Gioia, L. D. Dissecting the Intimate Mechanism of Cyanation of {2Fe3S} Complexes Related to the Active Site of All-Iron Hydrogenases by DFT Analysis of Energetics, Transition States, Intermediates and Products in the Carbonyl Substitution Pathway. *Chem.−Eur. J.* **2005**, *11*, 509−520.

(21) Zhou, T.; Mo, Y.; Liu, A.; Zhou, Z.; Tsai, K. R. Enzymatic Mechanism of Fe-Only Hydrogenase: Density Functional Study on H−H Making/Breaking at the Diiron Cluster with Concerted Proton and Electron Transfers. *Inorg. Chem.* **2004**, *43*, 923−930.

(22) Zhou, T.; Mo, Y.; Zhou, Z.; Tsai, K. R. Density Functional Study on Dihydrogen Activation at the H Cluster in Fe-Only Hydrogenases. *Inorg. Chem.* **2005**, *44*, 4941−4946.

(23) Zilberman, S.; Stiefel, E. I.; Cohen, M. H.; Car, R. Theoretical Studies of [FeFe]-Hydrogenase: Structure and Infrared Spectra of Synthetic Models. *J. Phys. Chem. B* **2006**, *110*, 7049−7057.

(24) Perdew, J. P.; Yue, W. Accurate and Simple Density Functional for the Electronic Exchange Energy: Generalized Gradient Approximation. *Phys. Rev. B: Condens. Matter Mater. Phys.* **1986**, *33*, 8800−8802.
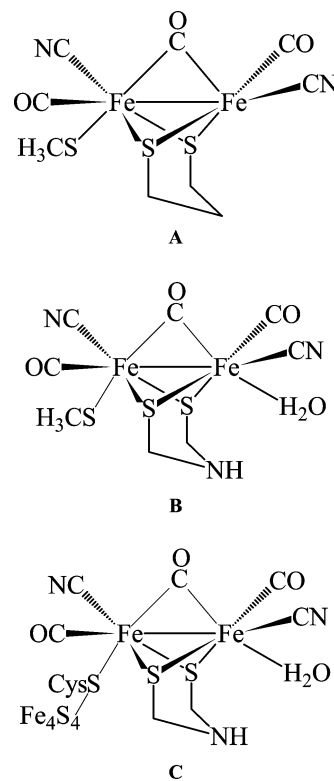
(25) Becke, A. D., Density-Functional Exchange-Energy Approximation with Correct Asymptotic Behavior. *Phys. Rev. A: At., Mol., Opt. Phys.* **1988**, *38*, 3098−3100.

(26) Hay, P. J.; Wadt, W. R. Ab Initio Effective Core Potentials for Molecular Calculations. Potentials for K to Au Including the Outermost Core Orbitals. *J. Chem. Phys.* **1985**, *82*, 299−310.

(27) Lee, C.; Yang, W.; Parr, R. G. Development of the Colle-Salvetti Correlation-Energy Formula into a Functional of the Electron Density. *Phys. Rev. B: Condens. Matter Mater. Phys.* **1988**, *37*, 785−789.

(28) Becke, A. D. Density-Functional Thermochemistry. III. The Role of Exact Exchange. *J. Chem. Phys.* **1993**, *98*, 5648−5652.

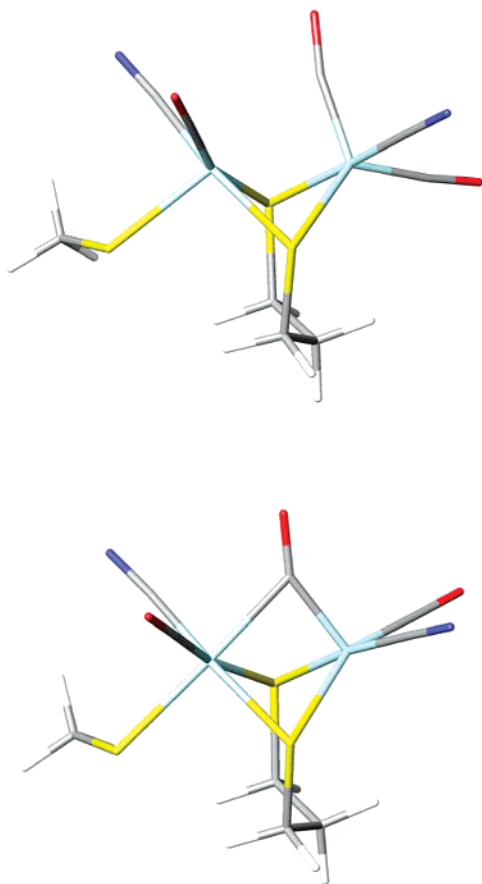(29) *Jaguar 7.0*, Schrodinger L.L.C.: Portland, OR 1991−2006.

Figure 3. Minimum energy conformations for the reduced form of **A**. Conformations for model compound **A** optimized at B3LYP/LACV3P** (a) and at BP86/LACV3P** (b). Conformation b is more tightly bridged with a Fe_p–CO distance of 2.181 Å, compared to 2.730 Å for a. Red, oxygen; yellow, sulfur; blue, nitrogen; aqua, iron; gray, carbon; and white, hydrogen.

were each changed to cyano groups, which is consistent with spectroscopic evidence[30-32] and with the presence of these groups ligated to the Fe atom in the active site of [Ni–Fe]-hydrogenase.[33] (2) The two sulfur atoms in $[2Fe]_H$ were bridged with dimethylamine ($-CH_2-NH-CH_2-$). (This bridge essentially replaced the second lone oxygen atom in the CpI crystal structure[4] whose original assignment was made in lieu of unresolved atoms bridging the sulfur atoms.) This bridging moiety has been previously suggested[34] because it can better act as a base than propane, which was originally presumed. It is also probable that the bridging moiety is the same for both CpI and DdH.[9] For **A**, however, we used propane as the bridging moiety so that we could compare our results to previous work.[17] Note that we denote the noncysteinyl sulfur atoms in $[2Fe]_H$ with subscripts a or b signifying that they lie either above or below the plane defined by Fe_p, Fe_d, and the middle heavy atom in the bridging moiety.

(30) Pierik, A. J.; Hulstein, M.; Hagen, W. R.; Albracht, S. P. A Low-Spin Iron with CN and CO as Intrinsic Ligands Forms the Core of the Active Site in [Fe]-Hydrogenases. *Eur. J. Biochem.* **1998**, *258*, 572–578.

(31) Van der Spek, T. M.; Arendsen, A. F.; Happe, R. P.; Yun, S.; Bagley, K. A.; Stufkens, D. J.; Hagen, W. R.; Albracht, S. P. Similarities in the Architecture of the Active Sites of Ni-Hydrogenases and Fe-Hydrogenases Detected by Means of Infrared Spectroscopy. *Eur. J. Biochem.* **1996**, *237*, 629–634.

(32) De Lacey, A. L.; Stadler, C.; Cavazza, C.; Hatchikian, E. C.; Fernandez, V. M. FTIR Characterization of the Active Site of the Fe-Hydrogenase from Desulfovibrio desulfuricans. *J. Am. Chem. Soc.* **2000**, *122*, 11232–11233.

(33) Happe, R. P.; Roseboom, W.; Pierik, A. J.; Albracht, S. P. J. Biological Activation of Hydrogen. *Nature* **1997**, *385*, 126–126.

(34) Nicolet, Y.; Cavazza, C.; Fontecilla-Camps, J. C. Fe-Only Hydrogenases: Structure, Function and Evolution. *J. Inorg. Biochem.* **2002**, *91*, 1–8.

For **1–8**, the following additional modifications were made: (3) Following Zhou et al.,[22] a CH_3SH group was coordinated to each of the three tricoordinated Fe atoms in the Fe_4S_4 cubane. The CH_3-SH groups might serve to provide an approximate protein environment for the Fe_4S_4 cubane as well as to prevent coordination between the Fe_4S_4 cubane and the cysteine, which is not observed in the crystal. (4) The nitrogen atom on the cysteine was capped by a hydrogen, and the carbonyl was capped with an NH_2; that is, the nitrogen on the next residue in the sequence was included and capped with two hydrogens. The peptide bond between the cysteine and residue 504 is thereby maintained. Current model compounds could therefore be used in a quantum mechanical/molecular mechanical model, and results could be compared in a straightforward manner. For **5**, the bridging carbonyl was rotated ~180° and the Fe–C–O bond angle changed to 180°. For **6–8**, one or two hydrogen atoms were added as shown in Figure 3 in ref 9.

For **A** and **B**, molecular charges of −1, −2, and −3 were employed to simulate the oxidized, semireduced, and reduced forms. For **C**, molecular charges of +1, 0, and −1 were employed because of the presence of the $[4Fe4S]_H$ subcluster, which was shown experimentally to have a +2 charge.[19] Molecular charges for **1** and **2** are +1 and 0, respectively, and −1 for **3–8**. Spin states for the semireduced forms for **A**, **B**, and **C**, and for **6** are $^1/_2$; all others are 0. Geometry optimizations were performed using initial coordinates as described above but, in addition, starting from optimal geometries for compounds lying adjacent in Armstrong's scheme (Figure 3 in ref 9). Geometry optimizations were performed with nitrogen in the dimethylamine bridging moiety oriented toward Fe_p and toward Fe_d. For open-shell systems, both restricted-spin and unrestricted-spin calculations were performed. Geometries reported here correspond to the lowest-lying energy minima we found, except when the conformations differ substantially from the crystal structure, that is, those structures that display a root mean square difference (RMSD) greater than 1 Å. In some cases, we found isoenergetic optimal conformations.

Results and Discussion

In previous calculations of model compounds of $[2Fe]_H$, methods ranging from the gradient generalized approximation (GGA) x-c functional within DFT, for example, Perdew–Wang,[21,22] BP86,[35] to the hybrid B3LYP x-c functional[18] were used. In a study for a related model compound, it was attested recently that B3LYP would result in poorer agreement with experimental structures,[20] even though that group applied B3LYP in earlier work.[15-17] The geometry of the reduced form of **A** (Table 1) optimized at B3LYP/LACV3P** shows that a carbonyl group (CO_b) partially bridges the Fe_p and Fe_d atoms (see Figure 3), which is consistent with previous work,[17] and with the asymmetrical bridging inferred in the crystal structure of $[2Fe]_H$ in DdH. (Note: the initial assignment of an oxygen atom or water molecule as the bridging ligand for $[2Fe]_H$ in DdH was due to a mixture of reduced and oxidized states leading to the unresolved carbon atom.[7]) However, because it has been recently suggested that a nonhybrid GGA x-c functional may be more appropriate,[20] we also optimized geometries at BP86/LACV3P**, which effects distinct changes; in particular, a more tightly bridged structure results (see Figure 3 and Table 1), which is inconsistent with B3LYP-optimized geometries (either with ours or with the results of Bruschi et al.[17]) and with the asymmetrical bridging found in the crystal structure of $[2Fe]_H$ in DdH.[6] The Fe_p–Fe_d distance we find for the reduced state of **A** is very close to the value observed for CpI, even though this crystal structure is thought to be an oxidized state. The

(35) Boyke, C. A.; Rauchfuss, T. B.; Wilson, S. R.; Rohmer, M.-M.; Benard, M. [Fe2(Sr)2)(mu-CO)(CNMe)6]2+ and Analogues: A New Class of Diiron Dithiolates as Structural Models for the H_{ox}^{Air} State of the Fe-Only Hydrogenase. *J. Am. Chem. Soc.* **2004**, *126*, 15151–15160.

Table 1. Geometrical Parameters for the Reduced Form of Model Compound A, a Compound Similar to A,[21] and the Crystal Structure DdH[3]

geometrical parameter	B3LYP	BP86	PBE0	Bruschi et al.[17]	Cao et al.[18]	Zhou et al.[21]	DdH[3]
Fe−Fe	2.612 Å	2.594 Å	2.543 Å	2.655 Å	2.655 Å	2.571 Å	2.566 Å
$Fe_p−CN_p$	1.956	1.903	1.923	1.939	1.941	1.88	1.845
$Fe_p−CO_p$	1.748	1.720	1.727	1.733	1.730	1.74	1.712
$Fe_p−SCH_3$	2.451	2.440	2.382	2.406	2.415	2.19	2.505
$Fe_d−CN_d$	1.947	1.899	1.911	1.933	1.934	1.88	1.865
$Fe_d−CO_d$	1.742	1.714	1.717	1.725	1.727	1.74	1.797
$Fe_d−CO_b$	1.758	1.802	1.740	1.754	1.794	1.746	2.494[a]
$Fe_p−CO_b$	2.730	2.181	2.559	2.638		2.921	2.807[a]
$Fe_p−S_a$	2.384	2.396	2.346	2.387		2.28	2.304
$Fe_p−S_b$	2.402	2.410	2.355	2.396	2.400	2.28	2.290
$Fe_d−S_a$	2.408	2.384	2.353	2.404	2.403	2.28	2.279
$Fe_d−S_b$	2.400	2.346	2.351	2.390		2.28	2.298
$Fe_d−C−O$	167°	149°	165°	∼164°			
ϕ_{CO}[b]	−156	−171	−159	−157[c]			174°[a]

[a] The oxygen atom originally assigned as the bridging moiety in the DdH crystal structure was used in lieu of CO_b. Note: the initial assignment of an oxygen atom (or water molecule) as the bridging ligand for $[2Fe]_H$ in DdH was due to a mixture of reduced and oxidized states leading to the unresolved carbon atom.[7] [b] ϕ_{CO} is defined in the text. [c] As specified by Bruschi et al.,[17] this value was measured as the rotation of the CO group with respect to the plane defined by Fe_p, Fe_d, and the midpoint between S_a and S_b, which we've found to be nearly identical to our definition.

Table 2. Partial Charges from a Natural Bond Order[38] Population Analysis for the Reduced Form of A Calculated with Different Functionals

	Bruschi et al.[17]	B3LYP	BP86	PBE0
Fe_p	−0.022	0.0045	−0.276	−0.126
Fe_d	−0.249	−0.263	−0.343	−0.352
SCH_3	−0.530	−0.613	−0.548	−0.575
$S_2C_3H_6$	−0.612	−0.689	−0.525	−0.601
CO_b	−0.208	−0.145	−0.154	−0.137
CO_d	−0.204	−0.153	−0.103	−0.128
CN_d	−0.565	−0.565	−0.536	−0.549
CO_p	−0.019	0.0200	0.0189	0.0487
CN_p	−0.591	−0.601	−0.535	−0.582

optimal molecular geometry obtained for fully reduced **A** by Cao and Hall,[18] who employed B3LYP with a mixed basis set, displays no carbonyl bridging Fe_p and Fe_d. Interestingly, the optimal geometry for a compound similar to **A** (but with a CH_3-SH ligand instead of CH_3S^- and, therefore, a −2 charge instead of −3) reported by Zhou et al.,[21] who used PW92[36] with a basis set of double-ζ quality, has values for $Fe_d−CO_b$ and $Fe_p−CO_b$ distances of 1.746 and 2.921 Å. Indeed, although Zhou et al.[22] have also extended their calculations to include the $[4Fe-4S]_H$ subcluster, it is difficult to assess the accuracy of their results because they were obtained with a smaller basis set and the PW x-c functional. The hybrid x-c functional PBE0[37] yields an optimal geometry more similar to the semibridged B3LYP structure than to the tightly bridged BP86 conformation. The sensitivity of the x-c functionals is demonstrated by comparison of the partial atomic charges calculated using a natural bond order[38] population analysis (see Table 2).

The oxidized and semireduced forms of **A** do not fit into Armstrong's scheme[9] and are only of interest in terms of a biomimetic system because **A** lacks a water ligand, as observed in the CpI crystal structure. For semireduced **A**, we obtained bridged and unbridged optimal conformations, in agreement with Bruschi et al.[17] For B3LYP and PBE0, the unbridged conforma-

tions are lower in energy by about 4.3 kcal/mol; for BP86, the unbridged conformation is lower by about 2 kcal/mol. Geometrical parameters are presented in Table 3 and compare reasonably well with the CpI crystal structure. The most notable difference is that the $Fe_p−Fe_d$ distances in the unbridged conformations obtained with B3LYP and PBE0 are 0.17 and 0.9 Å longer than observed in the CpI crystal structure. The molecular geometries we obtained with restricted-spin calculations are very similar to the unrestricted-spin results in Table 3, but the restricted-spin geometries are 6.6 and 7.6 kcal/mol higher in energy than the unrestricted-spin B3LYP- and PBE0-optimized structures, respectively. For all three functionals, $<S^2>$ values (where S is the total electron spin for the molecule) for the bridged conformations are about 0.8, in good agreement with the value expected for one unpaired electron, indicating only minor spin contamination. However, $<S^2>$ values are 1.6, for the unbridged conformations obtained with B3LYP and with PBE0, which indicates additional spin contamination (one would expect $<S^2>$ to be 3.75 for additional unpaired electrons), although for BP86, $<S^2>$ for both the bridged and unbridged structures is less than 0.8.

BP86 geometry optimizations for the oxidized form of **A** (Table 4), when starting with both bridged and unbridged geometries, resulted only in bridged structures, while applying B3LYP and PBE0 yielded both bridged and unbridged structures with the bridged structure lower in energy by 0.81 and 4.2 kcal/mol, respectively, for the two functionals. The unbridged B3LYP and PBE0 structures have large $Fe_p−Fe_d$ separations—3.198 and 3.078 Å, respectively—although the axial carbonyl is rotated to almost the same degree as in the bridged structures, that is, ϕ_{CO} = 173°. In contrast, Bruschi et al.,[17] employing B3LYP, found only a bridged conformation for oxidized **A**. It appears that the B3LYP/LACV3P** level of theory is able to locate the two local minima on the potential energy surface for the oxidized form of **A** corresponding to the bridged and unbridged conformations, while B3LYP with the mixed basis set used by Bruschi et al.[17] and BP86/LACV3P** are not. It is also notable that the $Fe_p−CO_b$ distance is shorter than $Fe_d−CO_b$ in the bridged structures we obtained with B3LYP, PBE0, and BP86, in agreement with the B3LYP-optimized geometries obtained by Bruschi et al.[17]

Model compound **B** with molecular charges of −1, −2, and −3 and model compound **C** with molecular charges of +1, 0, and −1 are analogous to the first two compounds in Armstrong's scheme[9] and one additionally oxidized form, that is, compounds

(36) Perdew, J. P.; Chevary, J. A.; Vosko, S. H.; Jackson, K. A.; Pederson, M. R.; Singh, D. J.; Fiolhais, C. Atoms, Molecules, Solids, and Surfaces: Applications of the Generalized Gradient Approximation for Exchange and Correlation. *Phys. Rev. B: Condens. Matter Mater. Phys.* **1992**, *46*, 6671−6687.

(37) Ernzerhof, M.; Scuseria, G. E. Assessment of the Perdew−Burke−Ernzerhof Exchange-Correlation Functional. *J. Chem. Phys.* **1999**, *110*, 5029−5036.

(38) *NBO 5.0*; Glendening, E. D., Badenhoop, J. K., Reed, A. E., Carpenter, J. E., Bohmann, J. A., Morales, C. M., Weinhold, F. Theoretical Chemistry Institute, University of Wisconsin: Madison, WI, 2001.

Table 3. Geometrical Parameters for the Semi-Reduced Form of A and the Crystal Structure CpI[4]

geometrical parameter	bridged				unbridged				CpI[4]
	B3LYP	BP86	PBE0	Bruschi et al.[17]	B3LYP	BP86	PBE0	Bruschi et al.[17]	
Fe−Fe	2.592	2.563	2.532	2.597 Å	2.791 Å	2.538 Å	2.706 Å	2.587 Å	2.617 Å
$Fe_p−CN_p$	1.943	1.903	1.911	1.927	1.985	1.924	1.960	1.958	1.857[a]
$Fe_p−CO_p$	1.766	1.740	1.744	1.768	1.779	1.741	1.759	1.757	1.754
$Fe_p−SCH_3$	2.389	2.370	2.341	2.337	2.402	2.288	2.355	2.335	2.378
$Fe_d−CN_d$	1.946	1.912	1.919	1.916	1.943	1.909	1.912	1.930	1.863[a]
$Fe_d−CO_d$	1.766	1.740	1.744	1.772	1.786	1.754	1.763	1.770	1.831
$Fe_d−CO_{b/axial}$	1.930	1.926	1.927	1.878	1.793	1.747	1.770	1.750	2.043
$Fe_p−CO_b$	2.082	1.976	2.003	2.116					2.100
$Fe_p−S_a$	2.405	1.363	2.357	2.379	2.418	2.324	2.383	2.372	2.319
$Fe_p−S_b$	2.410	2.388	2.360	2.386	2.354	2.346	2.314	2.355	2.340
$Fe_d−S_a$	2.380	2.348	2.336	2.375	2.361	2.304	2.314	2.312	2.337
$Fe_d−S_b$	2.363	2.321	2.319	2.371	2.376	2.323	2.331	2.355	2.320
$Fe_d−C_b−O_b$	142°	138°	140°						138°
$\phi_{CO}{}^b$	172	173	173		−9°	−13°	−9°		178[c]

[a] The CN ligands are assigned as CO ligands in the CpI crystal structure. [b] ϕ is defined in the text. [c] For the CpI active site, the midpoint between the two sulfur atoms was used to define ϕ_{CO}.

Table 4. Geometrical Parameters for the Oxidized Form of A and the Crystal Structure CpI[4]

geometrical parameter	bridged				unbridged		CpI[4]
	B3LYP	BP86	PBE0	Bruschi et al.[17]	B3LYP	PBE0	
$Fe_e−Fe_e$	2.519 Å	2.507 Å	2.468 Å	2.516 Å	3.198 Å	3.078 Å	2.617 Å
$Fe_p−CN_p$	1.936	1.902	1.906	1.923	1.932	1.908	1.857[a]
$Fe_p−CO_p$	1.802	1.769	1.776	1.789	1.768	1.749	1.754
$Fe_p−SCH_3$	2.325	2.344	2.287	2.312	2.297	2.263	2.378
$Fe_d−CN_d$	1.927	1.881	1.902	1.914	1.927	1.901	1.863[a]
$Fe_d−CO_d$	1.811	1.762	1.786	1.797	1.818	1.790	1.831
$Fed−CO_{b/axial}$	2.053	2.056	2.046	2.004	1.774	1.756	2.043
$Fe_p−CO_b$	1.911	1.857	1.866	1.929	3.315	3.193	2.100
$Fe_p−S_a$	2.370	2.353	2.324	2.367	2.355	2.299	2.319
$Fe_p−S_b$	2.371	2.333	2.325	2.352	2.402	2.337	2.340
$Fe_d−S_a$	2.335	2.274	2.298	2.338	2.362	2.322	2.337
$Fe_d−S_b$	2.333	2.213	2.298	2.339	2.384	2.349	2.320
$Fe_d−C_b−O_b$	134°	128°	133°		177°	177°	138°
$\phi_{CO}{}^b$	174	172	175		173	173	178[c]

[a] The CN ligands are assigned as CO ligands in the CpI crystal structure.[4] [b] ϕ_{CO} is defined in the text. [c] For the CpI active site, the midpoint between the two sulfur atoms was used to define ϕ_{CO}.

1, **2**, and **3**. Molecular geometries optimized at B3LYP/LACV3P** were all found to display a carbonyl (CO_b) bridging Fe_p and Fe_d, in agreement with Armstrong.[9] It appears that the water ligand in **B** and **C** precludes the unbridged structures observed for **A**. Geometrical parameters agree with the crystal structures (see the Supporting Information) with two exceptions. For the oxidized form of **B**, the separation between Fe_d and the water ligand is 0.9 Å shorter than in the CpI crystal structure. However, the first reduction increases Fe_d−water separation by 0.14 Å, and the second reduction increases it by an additional 0.3 Å, which is consistent with the departure of the water ligand from the active site upon reduction. For **C**, Fe_d−water separation is longer than that in the CpI crystal structure by 0.9 Å for all three charge states. In addition, compound **C** displays a close contact between the carbonyl oxygen in the cysteine and an Fe atom in the [4Fe−4S]$_H$ subcluster. This contact, which is not observed in the crystal structures, results from the deformation of dihedral angles from the values observed in the crystal and is prevented from occurring in model compounds **1**−**8** by the CH_3SH groups appended to [4Fe−4S]$_H$. The frontier molecular orbitals for the three charge states of **C** (see Figure 4) are localized on both the [4Fe−4S]$_H$ and [2Fe]$_H$ subclusters as well as on the sulfur bridge. In addition, the total spin density for semireduced **C** resides mostly on [4Fe−4S]$_H$ and only partially on [2Fe]$_H$ (see Figure 4), in contrast to results reported by Zhou et al.,[21] who found that the total spin density resides on [2Fe]$_H$ for a model compound that excludes [4Fe−4S]$_H$. It is therefore obvious that the [4Fe−4S]$_H$ subcluster must be included in model compounds for the [Fe−Fe]-hydrogenase active site if further mechanistic details are to be discerned.

Geometrical parameters for compounds **1**−**8** are presented in Table 5. Agreement between the crystal structures and the optimal geometries is good except that the distance between Fe_d and the water ligand in the CpI crystal structure is 0.8 Å longer than in **1**−**3**, which can be explained by other forces in the crystal acting on the water molecule. Our results agree with those reported by Schwab et al.,[39] who reported for [2Fe]$_H$ an Fe_p−Fe_d separation of 2.55 Å and Fe−S distances in the range of 2.33−2.35 Å for a structure composed of [4Fe−4S]$_H$ and [2Fe]$_H$ (but with a propane bridging the sulfurs in [2Fe]$_H$) and optimized with BP86 and a triple-ζ quality basis set. Optimal conformations for **1**−**8** are shown in Figure 5 in the same relation to each other as outlined by Armstrong.[9] However, we found for several species other conformations that were nearly isoenergetic or only slightly higher in energy than the ones displayed in Figure 5; for **3**, **4**, and **5**, conformations with the dimethyl amine bridge flipped toward Fe_d are only 0.2, 4.6, and 0.2 kcal/mol higher in energy, respectively. For the most part, Figure 5 follows Armstrong's scheme, but the exceptions are notable. The optimal conformation we found for **2** (and that also displayed a small RMS difference with the CpI crystal

(39) Schwab, D. E.; Tard, C.; Brecht, E.; Peters, J. W.; Pickett, C. J.; Szilagyi, R. K. On the electronic structure of the hydrogenase H-cluster. *Chem. Commun.* **2006**, *35*, 3696−3698.
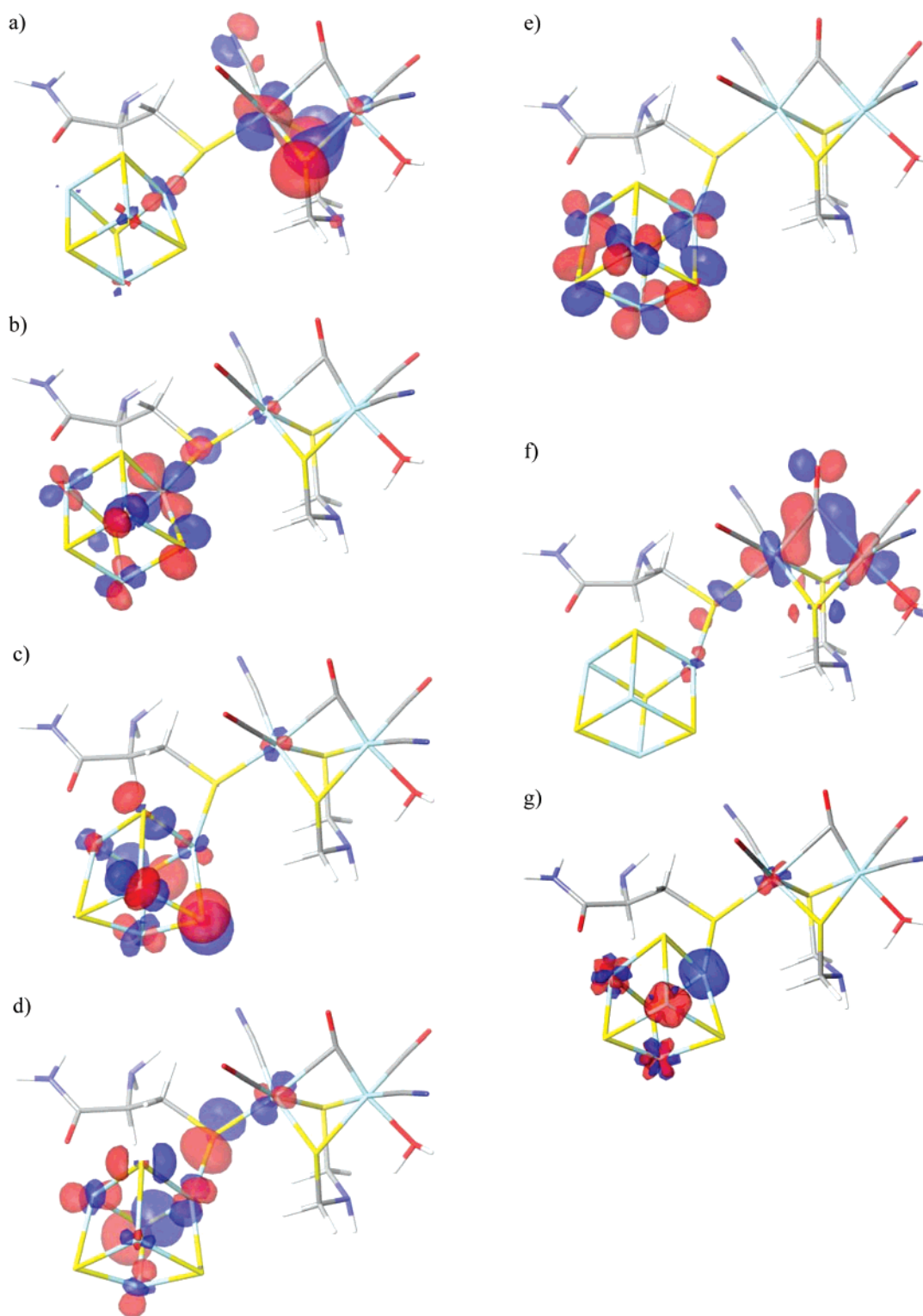
Figure 4. Frontier orbitals and total spin denisty for model compound **C**. The HOMO and the LUMO are displayed in a and in b, respectively, for the oxidized form (a molecular charge of +1) of model compound **C**. The HOMO and LUMO for the partially reduced form (a molecular charge of 0) of **C**, calculated with unrestricted-spin, are shown in c and d, respectively. The HOMO and LUMO for the reduced form (a molecular charge of −1) are shown in e and f. Total spin density is plotted for partially reduced **C** in g. Color legend for atoms is as follows: red, oxygen; yellow, sulfur; blue, nitrogen; aqua, iron; gray, carbon; and white, hydrogen.

structure) shows a carbonyl bridging Fe_p and Fe_d (indicated by an arrow in Figure 5) but the Fe_p−CO_b distance (1.833 Å) is shorter than the Fe_d−CO_b distance (2.457 Å). An optimal conformation 16 kcal/mol higher in energy has both Fe−CO_b distances almost equal, about 2.0 Å. We found that the equilibrium between **4** and **5** is not between bridged and

unbridged conformations (as displayed in Figure 3 in ref 9); **4** is semibridged, with an Fe_p−CO_b distance of 2.800 Å and ϕ_{CO} equal to 173°, while in **5**, the CO_b group has rotated away (ϕ_{CO} = 134°), resulting in an Fe_p−CO distance of 3.750 Å. However, the distance between Fe_d and the carbonyl coordinated primarily to Fe_p is 2.654 Å, and the dihedral corresponding to ϕ_{CO} (ϕ_{CO}'

Table 5. (a) Geometry Parameters for Compounds 1−6 and (b) Geometry Parameters for Model Compounds 7 and 8, and for Two Similar Model Compounds Due to Zhou et al.[22]

				Part a			
bond	CpI[4]	1	2	3	4	5	6
Fe−Fe	2.617	2.592	2.710	2.552	2.756	2.651	2.565
Fe_p-CN_p	1.857[a]	1.933	1.926	1.934	1.933	1.917	1.954
Fe_p-CO_p	1.754	1.800	1.806	1.795	1.788	1.766	1.806
Fe_p-S_{cys}	2.378	2.312	2.423	2.345	2.309	2.191	2.425
Fe_d-CN_d	1.863[b]	1.929	1.954	1.945	1.912	1.940	1.815
Fe_d-CO_d	1.831	1.842	1.821	1.817	1.814	1.814	1.800
$Fe_d-CO_{b/axial}$	2.043	1.869	2.457	1.932	1.774	1.761	1.804
Fe_d-OH_2	2.959	2.125	2.192	2.112			
Fe_p-CO_b	2.100	2.273	1.833	2.098	2.800	3.750	
Fe_p-S_a	2.319	2.332	2.394	2.351	2.335	2.367	2.381
Fe_p-S_b	2.340	2.346	2.416	2.343	2.322	2.367	2.346
Fe_d-S_a	2.337	2.381	2.335	2.357	2.347	2.281	2.350
Fe_d-S_b	2.320	2.365	2.341	2.349	2.360	2.291	2.362
$S_{cys}-Fe'_{cubane}$	2.321	2.176	2.372	2.286	2.232	2.273	2.425
$F_{ed}-C_b-O_{b/axial}$	138°	155°	121°	146°	172°	178°	178°
ϕ_{CO}[b]	178[c]	174	−176	172	173	6[d]	17

			Part b		
bond	**7a**	**7b**	**8**	1a[1]$_{ox}$[e]	1a[0]$_s$[e]
Fe−Fe	2.578	2.595	2.672	2.564	2.577
Fe_p-CN_p	1.820	2.029	1.932	1.926	1.912
Fe_p-CO_p	1.800	1.817	1.812	1.768	1.765
Fe_p-S_{cys}	2.357	2.387	2.380	2.269	2.283
Fe_d-CN_d	1.931	1.934	1.935	1.864	1.870
Fe_d-CO_d	1.788	1.797	1.813	1.779	1.768
Fe_d-CO_{axial}	1.786	1.785	1.762	1.764	1.756
Fe_p-S_a	2.383	2.336	2.387	2.263	2.278
Fe_p-S_b	2.396	2.393	2.423	2.284	2.294
Fe_d-S_a	2.357	2.338	2.310	2.243	2.249
Fe_d-S_b	2.359	2.352	2.329	2.252	2.260
$S_{cys}-Fe'_{cubane}$	2.325	2.327	2.317	2.158	2.165
Fe_p-H'		1.617	1.574	1.635	1.599
Fe_p-H''	1.630	1.633	1.687	1.642	1.633
Fe_d-H''	1.656	1.678	1.902	1.681	1.681
$H'-H''$	4.180	1.699	0.882	1.713	1.685
NC−H'		1.179	1.874	1.207	1.234
ϕ_{CO}[b]	11°	11°	12°	10°	10°

[a] The CN ligands are assigned as CO ligands in the CpI crystal structure. [b] ϕ_{CO} is defined in the text. [c] For the CpI active site,[4] the midpoint between the two sulfur atoms was used to define ϕ_{CO}. [d] The dihedral $N-Fe_p-Fe_d-CO_p$ is 176°. [e] Notation used for the model compounds in the last two columns is the same as in ref 22. 1a[1]$_{ox}$ and 1a[0]$_s$ are oxidized and semi-reduced and have charges of +1 and 0, respectively.

= NH−Fe_p−Fe_d−CO) is 176°, so that **5** can also be considered to be in a semibridged conformation but with Fe_p and Fe_d bridged by a different carbonyl—the one coordinated only to Fe_p in **4**. Model compound **5** is lower in energy than **4** by 12.4 kcal/mol.

The question of whether the organic ligand bridging the sulfurs in [2Fe]$_H$, here dimethylamine, acts as a base in the addition of a hydrogen atom to model compound **5** was posed by Armstrong.[9] Although we did indeed find an optimal conformation for model compound **6** in which the dimethylamino group is protonated, it is 65 kcal/mol higher in energy than the lowest-energy conformation we found. The energetically preferred location of the first added hydrogen atom in Armstrong's scheme[9] is the nitrogen of the cyano group coordinated to Fe_d (see Figure 5). We also found for model compound **6** an optimal conformation with a hydride bridging Fe_p and Fe_d, but this, too, is about 65 kcal/mol higher in energy than the lowest-energy conformation. For model compound **7**, formed when a second hydrogen atom is added, we considered all combinations of two hydrogen atoms attached to the cyano ligands (to both the carbons and the nitrogens), to the nitrogen in the dimethylamino bridge, and to Fe_p and Fe_d via a hydride bridge. As shown in Figure 5, the lowest-energy conformation, labeled **7a**, has a hydride bridge and a hydrogen atom bonded to the nitrogen of the cyano ligand coordinated to Fe_p. A conformation 9.2 kcal/mol higher in energy has a hydride bridge

and a hydrogen atom bonded to the nitrogen of the dimethylamino bridge, although it is unclear how this conformation is involved in the formation of molecular hydrogen. Another higher-energy conformation that does appear to be involved in H_2 formation is labeled **7b** in Figure 5; it is similar to model compound **7a** except that the hydrogen originally bonded to the nitrogen atom in the cyano ligand coordinated to Fe_p has migrated to the cyano ligand's carbon atom and is separated from the hydride by only 1.7 Å. Model compound **7b** is 20.4 kcal/mol higher in energy than **7a** but only 2.3 kcal/mol lower in energy than model compound **8**, which has H_2 coordinated to Fe_p. A conformation 2.6 kcal/mol higher in energy than **8** has the NH in the dimethyl amine flipped toward Fe_d. Zhou et al.,[22] using the same model compound, obtained a structure similar to **7b** but only for the oxidized and semireduced states, that is, with charges of +1 and 0, and did not find an optimal geometry with H_2 coordinated to Fe_p, as in our model compound **8**, for any charge state. Superimposing either model compound **7b** or **8** with the CpI crystal structure for [2Fe]$_H$, [4Fe−4S]$_H$, and the cysteine linking them, we found RMS differences of 0.74 and 0.66 Å, respectively. (For this calculation, we changed two of the CO groups in the CpI structure to CN, and we included only atoms that were common to both the crystal structure and the model compounds. In addition, we did not include the bridging CO in the crystal structure and the corresponding CO in the model compounds, which is rotated
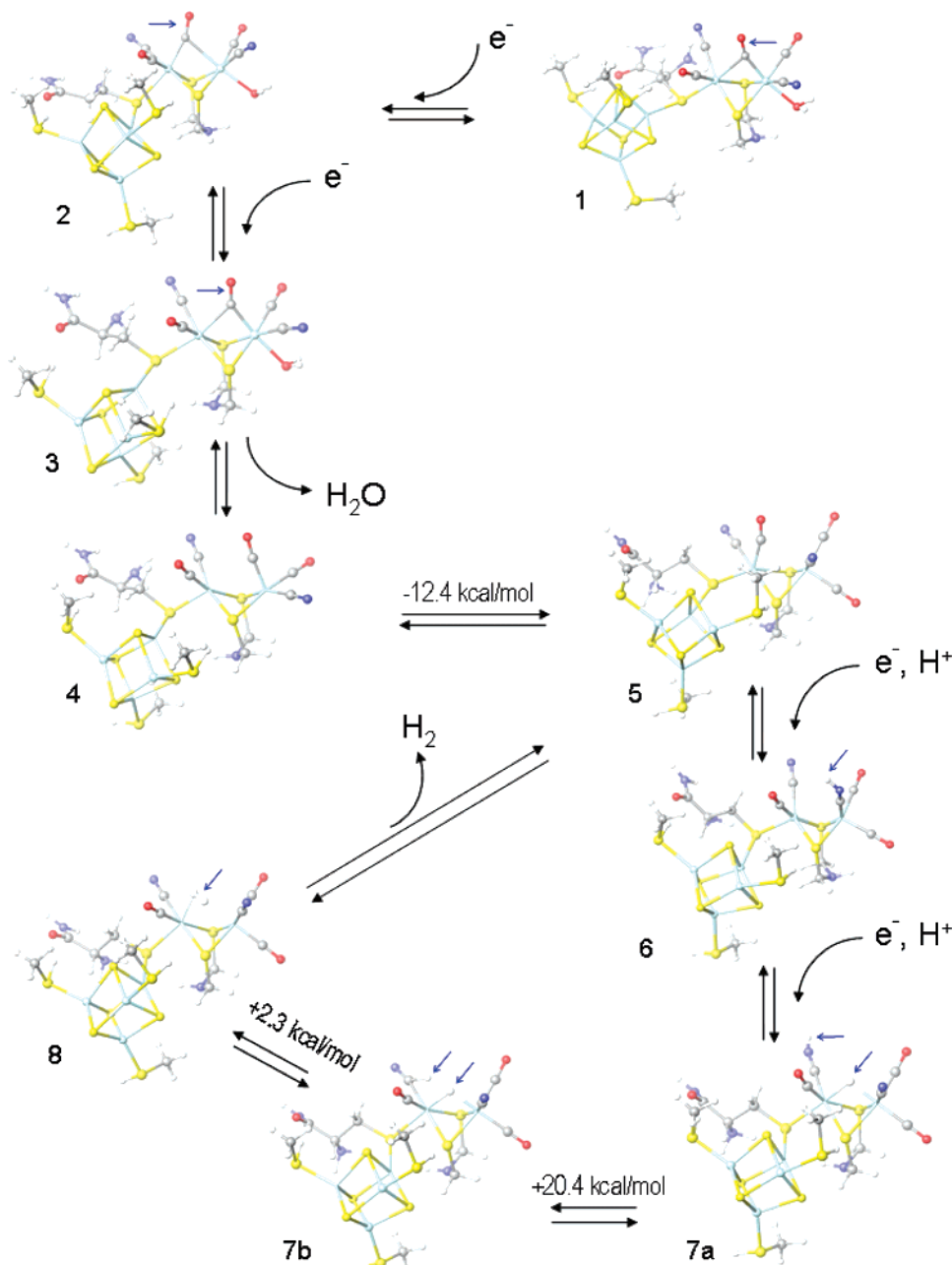
7

Figure 5. Optimal conformations of model compounds **1**−**8** inserted into Armstrong's scheme.[9] Blue arrows were drawn to indicate significant structural features.

~180°.) Superposition of **8** with the CpI crystal structure[4] is shown in Figure 6. The largest difference is in the shape and orientation of the [4Fe−4S]$_H$ subcluster, which is much closer to a perfect cube in **8** than in the crystal structure. The difference in orientation is due to coordination between the cysteine's carbonyl group and one of the CH$_3$SH groups.

Plots of the highest occupied and lowest unoccupied molecular orbitals (HOMO and LUMO, respectively) for **7b** and **8** (see Figure 7) are similar for the two species; the HOMO is localized on the [4Fe−4S]$_H$ and the LUMO on the [2Fe]$_H$. Using natural bond order analysis,[38] we found that for model compound **7b** the partial charge on the hydride bridging Fe$_p$ and Fe$_d$ is −0.06 while the partial charge on the hydrogen bound to CN$_p$ is +0.27. For model compound **8**, the partial charge on the hydrogen bound to CN$_p$ is +0.21, which is similar to model compound **7b**, and the partial charge for the other hydrogen atom in H$_2$ is +0.04. We removed the H$_2$ from model compound **8** and reoptimized the geometry, hoping to reobtain model
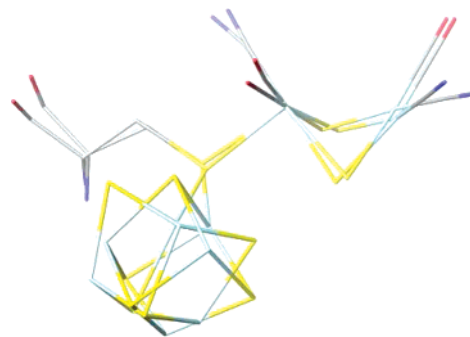

Figure 6. Superposition of model compound **8** with the active site from the CpI crystal structure. RMSD = 0.740 Å. Only common atoms were used and are shown, as described in the text. Red, oxygen; yellow, sulfur; blue, nitrogen; aqua, iron; and gray, carbon.

compound **5**. The resulting geometry was very close to model compound **5** except for a closer than usual contact (3.734 Å)
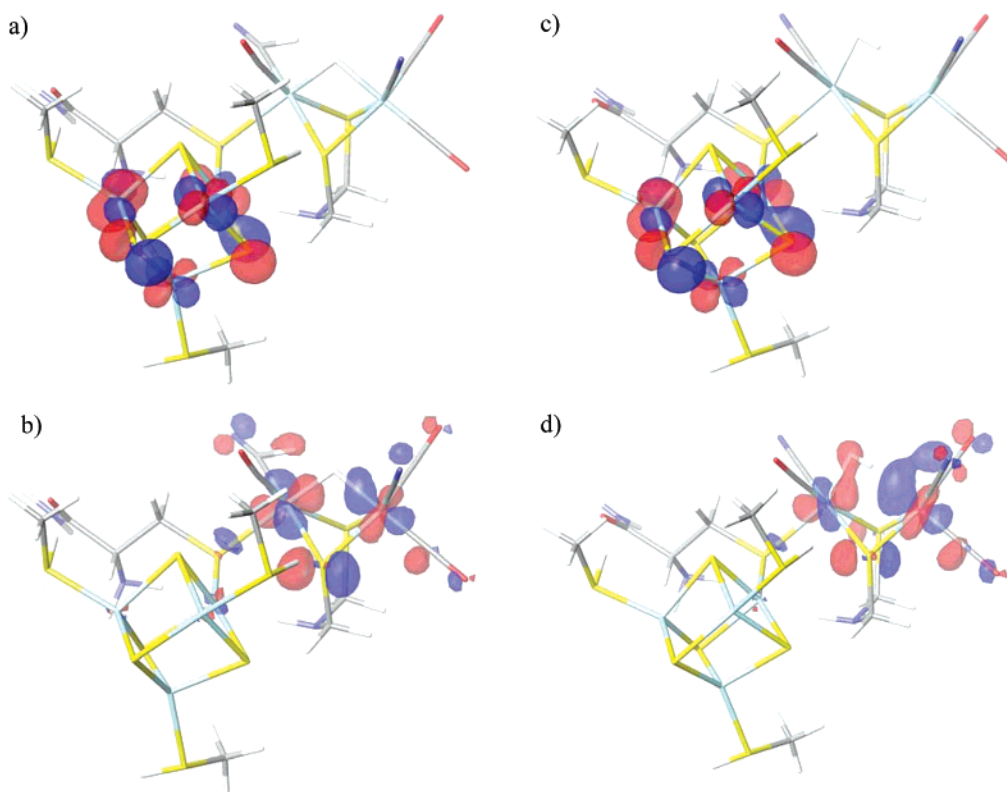
Figure 7. Frontier orbitals for model compounds **7b** and **8**: (a) HOMO for **7b**; (b) LUMO for **7b**; (c) HOMO for **8**; (d) LUMO for **8**. Color legend for atoms is as follows: red, oxygen; yellow, sulfur; blue, nitrogen; aqua, iron; gray, carbon; and white, hydrogen.

between a sulfur in $[2Fe]_H$ and the Fe atom in $[4Fe-4S]_H$ that is coordinated to the cysteinyl sulfur. Imposing our requirement that conformations must be reasonably close to the crystal structure, we rejected this conformation but do not believe that it is evidence that model compounds **8** and **5** do not represent species that are in equilibrium.

Conclusions

By comparing calculated to experimental structures for $[2Fe]_H$, we determined that B3LYP/LACV3P** is a more appropriate level of theory for investigating the mechanism of hydrogen production in [Fe-Fe]-hydrogenase. In addition, although almost all previous theoretical studies include only $[2Fe]_H$ in model compounds of the [Fe-Fe]-hydrogenase active site, we showed that the $[4Fe-4S]_H$ cluster in addition to $[2Fe]_H$ should be included because frontier orbitals are localized on both the $[4Fe-4S]_H$ and $[2Fe]_H$ subclusters as well as on the sulfur bridge linking the two subclusters. We also showed that

optimal geometries for some of the intermediates in a previous hypothesis by Armstrong[9] are somewhat different than previously thought. However, ours is the first theoretical confirmation of the fully reduced structure with transient H_2 bound to the proximal Fe atom. We have established a starting point for a future investigation of the effects of the protein environment on the catalytic mechanism of [Fe-Fe]-hydrogenases.

Supporting Information Available: Geometry parameters for model compounds **B** and **C**. This material is available free of charge via the Internet at http://acs.pubs.org

EF060577N